Nigerian Journal of Technology (NIJOTECH)
Vol. 32. No. 2. July 2013, pp. 363 – 367

University of Nigeria, Nsukka, ISSN 1115-8443
www.nijotech.com

INVESTIGATION OF SPATIAL DISTRIBUTION PROPERTIES OF MID-INFRARED QUANTUM CASCADE LASERS AT 7 μM

S. O. Edeagu,
NANOELECTRONICS RESEARCH GROUP, DEPARTMENT OF ELECTRONIC ENGINEERING, UNIVERSITY OF NIGERIA, NSUKKA, NIGERIA
sedeagu@yahoo.com

Abstract

The spatial distribution properties of quantum cascade lasers with emission wavelengths around 7 μm were measured. In addition, the emission profile on a plane orthogonal to the propagation axis of the beam were measured and the full width at half maximum (FWHM) on the orthogonal and lateral directions calculated. Both the monomode and multimode structures at different emission powers were tested, showing that the dispersion does not change significantly (in the range between 42° and 52° on the orthogonal direction and between 28° and 32° on the lateral direction). However, the multimode structure presents several local maxima, which makes it difficult to achieve an efficient collimation of the emitted optical power. The results can be used to design a dedicated optical system to collimate and focus the emission from quantum cascade lasers for spectroscopic applications.

Keywords: Semiconductor laser, Quantum cascade laser, Mid-infrared, Spatial Distribution, Distributed feedback structures, Spectroscopy

1. Introduction

Quantum cascade lasers (QCLs) [1] operating at room temperature in the mid-infrared spectral region (3.4 – 17 μm) have been found useful for several applications including environmental sensing, pollution monitoring, medical applications [2], optical communications, mid-infrared spectroscopy [3 – 6] and more recently atomic physics spectroscopy [7]. One of the main issues related to the possible application of their performances is the ability to collect all the emitted optical power and to focus it onto a target, whose dimensions are comparable with the facet of the laser, or to feed in a cavity avoiding the occurrence of stray light [8]. In the case of a QCL emitting in the infrared region, one has to consider that the exploitable optics are quite expensive: materials like germanium (Ge), zinc selenide (ZnSe) and calcium fluoride (CaF_2) are involved, which require particular attention in designing optical items and are not suitable to be easily adapted once fabricated. Thus, it becomes important to define the actual spreading of their optical emission, both in terms of modal distribution and of power dispersion. This would allow for designing the proper optics to collimate the whole beam and to focus the power avoiding several steps of repeated attempts, which would result in increasing costs and fabrication times.

2. Experimental Setup

Two quantum cascade laser structures were used, one with a distributed feedback grating on the waveguide provided by Alpes Lasers, Switzerland [9] and the other, a basic structure without a distributed feedback grating, provided by the Walter Schottky Institut (WSI), Technische Universität München, Germany. The quantum cascade laser without a distributed feedback grating (basic structure) is composed of a bound-to-continuum active region embedded in a cavity acting as a Fabry-Pérot structure.

It has an emission wavelength of approximately 7 μm at and a relatively low optical emitted power of about 100 mW at cryogenic temperatures. The quantum cascade laser from Alpes Lasers is a pulsed distributed feedback laser with a power > 1W peak power at 1474 cm^{-1} (λ = 6.784 μm) at 110 K.

The distributed feedback structure [10] incorporate a grating structured at the surface of the laser ridge resulting in a narrow linewidth and monomodal behavior of the emitted radiation. This makes them suitable for spectroscopic applications which require precision on the emission wavelength and finer tunability. The basic laser structure without distributed feedback was used to compare the difference arising from multimode and monomode emission.

The lasers were mounted on small copper heatsinks which were then fixed on the cold finger of a temperature controlled liquid nitrogen (N_2) flow cryostat (Oxford Instruments OptistatDN-V). A commercial pulse generator (Avtech AVR-5B-B-PN-BR) provided the pulse to drive the laser. Typical pulsed operating conditions were 250 ns pulses with a 400 Hz repetition frequency, corresponding to a duty cycle of 10^{-4}. These conditions guaranteed that minimal device heating would occur during the single pulse. The emitted light of the lasers was coupled out of the cryostat through a CaF_2 lens window (f/1.0) with antireflection coating. The emission was detected using a liquid nitrogen cooled mercury cadmium telluride (HgCdTe) detector (Judson MCT J19D11), with a detection area of 2 x 2 mm^2, thus providing a virtual detection point. The detector was placed 35 mm from the window of the cryostat and thus 50 mm from the front facet of the QCL and perpendicular to the axis of the emission. In order to define the relative position of the laser emission, a sheet of graph paper divided into four quadrants with both the horizontal (x-axis) and the vertical (y-axis) axes ranging from -50 mm to +50 mm is placed slightly above the CaF_2 window of the cryostat. A pointer placed on top of the HgCdTe detector lid is thus used to mark the detector position and an x-y-z table positioned (Newport RS 4000) provides both vertical and horizontal displacement to move the detector along the x- and y-axis. The power dispersion on a plane orthogonal to the beam propagation was measured and the vertical and horizontal divergence of the laser emission was calculated. Fig. 1 shows a schematic of the experimental setup used to measure spatial distribution of QCLs. Since the laser is placed on the cold finger vertically, the horizontal dispersion corresponds to the actual orthogonal divergence (fast axis) and the vertical one corresponds to the actual lateral divergence (slow axis).

The resulting data was recorded on a 5 Gsample/s 2GHz bandwidth digital oscilloscope (LeCroy WaveRunner 6200A). Measurements were taken in steps of 2 mm by scanning from the 'origin' (0, 0) in both the horizontal and vertical directions and the optical power was recorded using a program module written using National Instruments' LabView 8.5. The measured positions were then analyzed using the Origin 7G graphing and analysis software and reported on 2D graphs to provide an immediate estimation of the power dispersion.

3. Results and discussion

A complete evaluation of the dispersion as a function of the position and of the emitted power has been performed on the DFB laser. The experimental results for the spatial distribution in the four quadrants at an emitted power corresponding to 60% of the maximum power are shown in Fig. 2 as an intensity plot. The divergence takes an elliptical shape. In order to define its magnitude, the area where the emission is more than 50% of the maximum (the area encircled by the dash line in Fig. 2) has been taken into account. The full width at half maximum (FWHM) on the horizontal angle is 42 ± 2° while the vertical one is confined to 28 ± 2°.

In order to show the dependence on the power in Fig. 3, the results of the central part of the emission corresponding to different values of the power, ranging from 3% to 80% of the maximum value, are reported. It is evident that the distribution does not change significantly. The fast axis divergence defined by the FWHM on the horizontal direction decreases slightly, going from
52 ± 3° for 3% of the power to 47 ± 3° at 40%

and 43 ± 2° at 80%. In addition, the area corresponding to the higher emitted power increases in comparison to the whole surface.

The divergence of the low power DFB laser has been measured in the area surrounding the point of maximum emission at a value corresponding to 60% of the maximum power and the results are reported in Fig. 4. The dispersion is similar to the one for the first laser in both the vertical and the horizontal direction, with FWHM for the fast axis of 43 ± 2° and for the slow axis of 32 ± 2°. This confirms that the dispersion is typical for such kind of laser.

In order to provide a comparison with the Fabry-Pérot structure, dispersion measurements at a power corresponding to 60% of the maximum were performed. The results are shown in Fig. 5. It is evident that the elliptical shape, with a FWHM of 50 ± 2° on the fast axis and 20 ± 2° on the slow axis, but including several local maxima are present, indicating the probable presence of interference effects related to a multimode emission. For an efficient collection of all the emitted power, a QCL without DFB grating is thus less suitable, since the presence of different modes occurring at the same time makes it difficult to collimate and focus all the modes simultaneously.

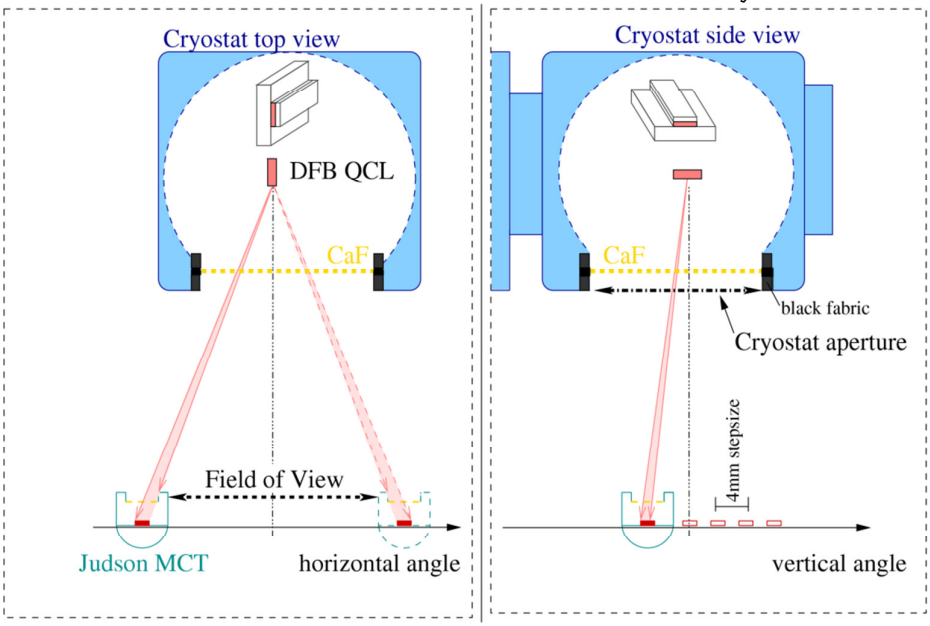

Fig. 1: Schematic of the experimental setup used to measure the spatial distribution. The laser is mounted orthogonal to the direction of propagation, thus the horizontal angle corresponds to the orthogonal divergence and the vertical one corresponds to the lateral one.

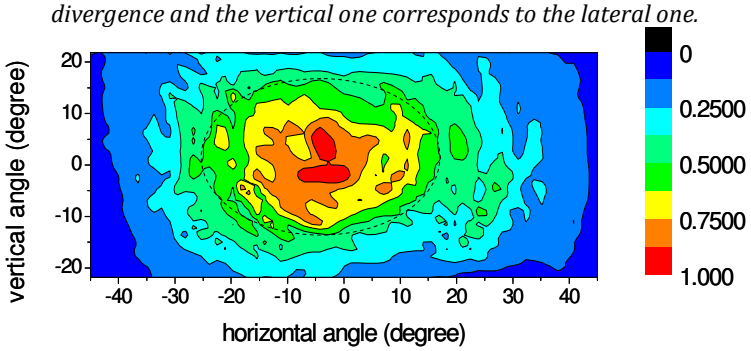

Fig. 2: Power dispersion of the high powered DFB laser emitting at 60% of its maximum power. The drawn ellipse (dash line) represents the area corresponding to more than 50% of the maximum. The beam divergence is 42° on the horizontal angle and 28° on the vertical one.

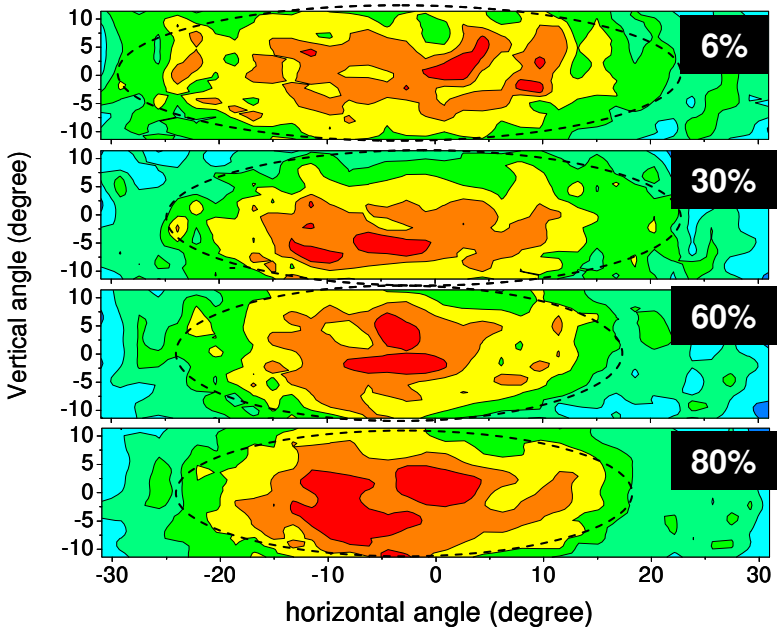

Fig. 3: Power dispersion of the high powered DFB laser emitting (from top to bottom) at 6%, 30%, 60% and 80% of its maximum power. The ellipses limited by the dashed lines correspond to the area where the power is more than 50% of the maximum.

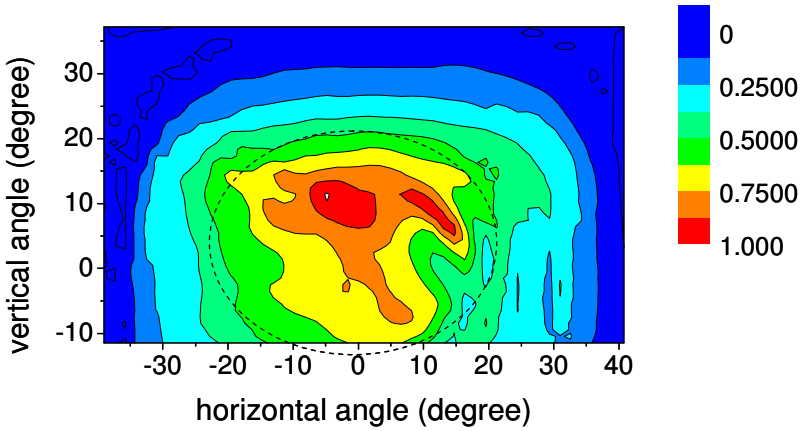

Fig. 4: Power dispersion of the low powered DFB laser. The divergence again has been defined by calculating the area where the optical power is more than 50% of the maximum.

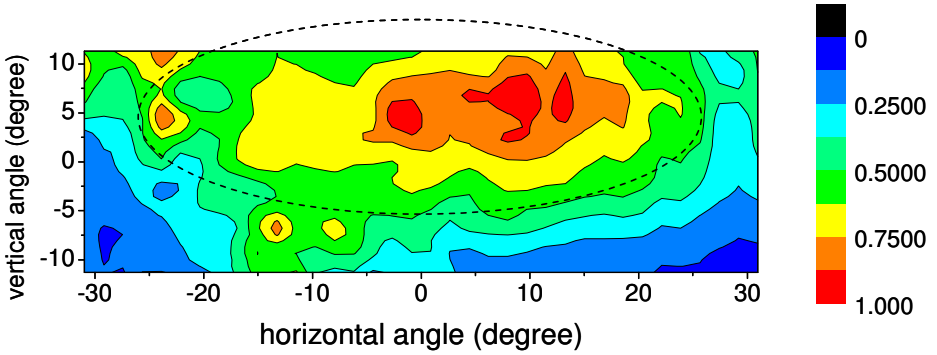

Fig. 5: Power dispersion of the Fabry-Pérot structure emitting at 60% of its maximum power. It is evident that several local maxima are present, hinting at some interference phenomena among the different modes.

4. Conclusion

In conclusion, the spatial distribution of different quantum cascade laser structures emitting around 7 μm were measured with the aim of verifying their performance in terms of possible utilization for atomic physics spectroscopic applications. The power dispersion on a plane orthogonal to the beam propagation was measured and therefore the vertical and horizontal divergence of the laser emission was calculated.

The distributed feedback structure and the basic structure were compared and it was shown that there were no significant differences in the divergence angles, indicating that it is mostly due to the intrinsic effect of the quantum cascade laser emission. However, in the basic structure the multimode emission gives rise to several local maxima, making it more difficult to provide efficient collection of the power with respect to the distributed feedback structure. We have shown that for an efficient collection of all emitted power, quantum cascade lasers without distributed feedback gratings are less suitable. This is due to the presence of different modes which occur at the same time thus making it different to colimate and focus the emitted power.

The comparison of DFB emission at different emitted powers presents no great difference, even narrowing the area where the emission is higher with increasing the power. The results obtained are typical of similar QCL structures and they could be used to design a dedicated and efficient optical system to perform atomic physics spectroscopy.

Acknowledgements

This work was carried out at the Institute for Nanoelectronics and the Walter Schottky Institut, Technische Universität München, Munich, Germany.

References

[1] Faist, J., Capasso, F., Sivco, D. L., Sirtori, C., Hutchinson, A. L. and Cho, A. Y. Quantum Cascade Laser. *Science*, Vol. 264, Number 5158, 1994, pp. 553 – 556.

[2] Edeagu, S.O. Mid-Infrared Quantum Cascade Lasers. *Nigerian J. of Technology*, Vol. 31, Number 3, 2012, pp. 228 – 232

[3] McManus, J.B., Nelson, D.D., Shorter, J.H., Jimenez, R., Herndon, S., Saleska, S., and Zahniser, M. A high precision pulsed quantum cascade laser spectrometer for measurements of stable isotopes of carbon dioxide, *Journal of Modern Optics*, Vol. 52, Number 16, 2005, pp. 2309 – 2321.

[4] Charlton, C., Temelkuran, B., Dellemann, G., and Mizaikoff, B. Midinfrared sensors meet nanotechnology: Trace gas sensing with quantum cascade lasers inside photonic band-gap hollow waveguides. *Appl. Phys. Lett.* Vol. 86, Issue 19, 2005, pp. 194102 – 194102-3.

[5] Wysocki, G., Curl, R.F., Tittel, F.K., Maulini, R., Billiard, J.M., and Fais, J. Widely tunable mode-hop free external cavity quantum cascade laser for high resolution spectroscopic applications. *Appl. Phys. B*. Vol. 81, Issue 6, 2005, pp. 769 – 777.

[6] Hvozdara, L., Pennington, N., Kraf, M., Karlowatz, M., and Mizaikoff, B. Quantum cascade lasers for mid-infrared spectroscopy. *Vibrational Spectroscopy*. Vol. 30, Issue 1, 2002, pp. 53–58.

[7] Vacchi, A., Regoliosi, P., Scarpa, G., and Lugli, P. Steps towards the development of a QCL laser for mμH experiments in Book of Abstracts, Intl. Conf. on Precision Physics of Simple Atomic Systems, Venice, Italy, 2006, p. 33.

[8] Krishnaswami, K., Bernacki, B.E., Cannon, B.D., Ho, N., and Anheier, N.C. Emission and Propagation Properties of Midinfrared Quantum Cascade Lasers. *IEEE Photon. Tech. Lett*. Vol. 20, Issue 4, 2008, pp. 306 – 308.

[9] Alpes Lasers SA, Neuchâtel, Switzerland: http://www.alpeslasers.ch/. Accessed on October 14, 2008.

[10] Hofstetter, D., Beck, M., Aellen, T., and Faist, J. High-temperature operation of distributed feedback quantum-cascade lasers at 5.3 μm. *Appl. Phys. Lett*. Vol. 78, Issue 4, 2001, pp. 396 – 398.